

# *Surface modification of natural vein graphite for the anode application in Li-ion rechargeable batteries*

**T. H. N. G. Amaraweera,  
N. W. B. Balasooriya,  
H. W. M. A. C. Wijayasinghe,  
A. N. B. Attanayake, B.-E. Mellander &**

**Ionics**

International Journal of Ionics The  
Science and Technology of Ionic Motion

ISSN 0947-7047

Ionics

DOI 10.1007/s11581-018-2523-5



# Ionics

International Journal  
of Ionics The Science  
and Technology of Ionic  
Motion

 Springer

 Springer

**Your article is protected by copyright and all rights are held exclusively by Springer-Verlag GmbH Germany, part of Springer Nature. This e-offprint is for personal use only and shall not be self-archived in electronic repositories. If you wish to self-archive your article, please use the accepted manuscript version for posting on your own website. You may further deposit the accepted manuscript version in any repository, provided it is only made publicly available 12 months after official publication or later and provided acknowledgement is given to the original source of publication and a link is inserted to the published article on Springer's website. The link must be accompanied by the following text: "The final publication is available at [link.springer.com](https://link.springer.com)".**



# Surface modification of natural vein graphite for the anode application in Li-ion rechargeable batteries

T. H. N. G. Amaraweera<sup>1,2</sup> · N. W. B. Balasooriya<sup>3</sup> · H. W. M. A. C. Wijayasinghe<sup>1</sup> · A. N. B. Attanayake<sup>2</sup> · B.-E. Mellander<sup>4</sup> · M. A. K. L. Dissanayake<sup>1</sup>

Received: 1 November 2017 / Revised: 27 February 2018 / Accepted: 4 March 2018

© Springer-Verlag GmbH Germany, part of Springer Nature 2018

## Abstract

Natural vein graphite with high purity and crystallinity is seldom used as anode material in lithium-ion rechargeable batteries (LIB) due to impurities and inherent surface structure. This study focuses on improving the surface properties of purified natural vein graphite surface by employing mild chemical oxidation. Needle-platy graphite sample with initial average carbon percentage of 99.83% was improved to 99.98% after treatment with 5 vol.% HCl. Surface modification of purified graphite was done by chemical oxidation with  $(\text{NH}_4)_2\text{S}_2\text{O}_8$  and  $\text{HNO}_3$ . Fourier-transform infrared spectra of graphite after chemical indicating surface oxidation of graphite surface. X-ray diffraction and scanning electron microscopic studies show the improvement of graphite structure without modification of crystalline structure. Electrochemical performance of lithium-ion cell assembled with developed anode material shows noticeable improvement of the reversible capacity and coulombic efficiency in the first cycle and cycling behavior after surface modification.

**Keywords** Vein graphite · Surface modification · Lithium-ion battery

## Introduction

Expensive electrode materials used in LIB lead to higher unit costs that hinder the development of LIB as a low-cost portable power source. Still, expensive porous carbon materials and synthetic graphite are the most commonly used anode materials in commercial LIB [1, 2]. Vein graphite is renowned for its high purity and crystallinity [3]. However, it is rarely used in electrochemical systems. Four structurally distinct vein graphite varieties, namely, shiny-slippery-fibrous graphite (SSF), needle-platy graphite (NPG), coarse striated-flaky graphite (CSF), and coarse flakes of radial graphite (CFR)

have been identified [2]. Each structural type consists of 95–99% of carbon. Impurity content in each structural type varies depending on the mode of occurrence and nature of the graphite vein [3, 4]. Those impurities are either mechanically attached to the graphite surface or intercalated between adjacent graphene layers.

The purity level in natural graphite normally required for electrochemical applications is in the range of < 0.1% ash with the accepted level of heavy metals < 10 ppm [1, 5]. Various thermal and chemical purification methods have been investigated to remove the mechanically attached and intercalated impurities in natural graphite with more than 98% of carbon [6–8]. Our previous study suggested a cost effective method for removing the impurities in vein graphite and upgrading the carbon content to 99.99% [9]. Chemical oxidation has been used to synthesize graphene oxide and anode materials for LIB from vein graphite [10–14]. The surface structure of graphite is a crucial factor for the formation of the solid electrolyte interface (SEI) layer and consequently its electrochemical performance in LIB [15–25]. Mild oxidation by thermal and chemical treatments has been identified as a successful method for surface modification [15–24]. Acid digestion technique that uses a combination of HF,  $\text{HNO}_3$ , and  $\text{H}_2\text{SO}_4$  acids has been used to purify vein graphite for the anode application

✉ H. W. M. A. C. Wijayasinghe  
athulawijaya@gmail.com

<sup>1</sup> National Institute of Fundamental Studies, Kandy, Sri Lanka

<sup>2</sup> Department of Science and Technology, Uva Wellassa University, Badulla, Sri Lanka

<sup>3</sup> Department of Geology, University of Peradeniya, Peradeniya, Sri Lanka

<sup>4</sup> Department of Applied Physics, Chalmers University of Technology, Göteborg, Sweden

of lithium-ion battery [13]. However, those methods, which used corrosive and expensive chemicals for the purification and modification, are unfavorable for practical applications. Therefore, this present work focuses on investigating the possibility of developing vein graphite as anode material in LIB by surface modification via chemical oxidation using low concentrated mineral acid and chemical oxidant in economically viable and eco-friendly approach.

## Experimental

### Purification

Needle-platy graphite (NPG) from Sri Lanka, with particle size  $< 53\ \mu\text{m}$  and carbon content 99.83%, was used for this study. Small chips of graphite were crushed in a vibratory disk mill for 3 to 4 min to form a powder. Particle size fraction  $< 53\ \mu\text{m}$  separated by mechanical sieving was used for the experiment. The raw graphite powders (3.75 g) were leached in aqueous solutions containing 5 vol.% HCl (25 ml) separately and heated to 60 °C for 75 min [9]. The acid-leached materials were washed to neutral. The material was dried under vacuum to remove moisture. The treated graphite was further leached by leached in aqueous solutions containing 5 vol.% HCl (25 ml) separately and heated to 60 °C for 75 min. The acid-leached materials were washed to neutral. The material was dried under vacuum to remove moisture.

### Surface modification

The modification of the purified graphite surface was carried out by chemical oxidation. Two strong oxidizing agents, hot concentrated  $\text{HNO}_3$  (NO method) and 1 M  $(\text{NH}_4)_2\text{S}_2\text{O}_8$  in 1 M  $\text{H}_2\text{SO}_4$  (NS method) were used for the chemical oxidation [16]. For the NO method, graphite powder (3 g) was reacted with 69%  $\text{HNO}_3$  solution (100 ml) at 60 °C for 24 h, followed by washing with distilled water until all the acid was removed. Then, the treated sample was dried under vacuum. The modification of graphite powder by the NS method was carried out by treating graphite powder (3 g) with 1 M  $(\text{NH}_4)_2\text{S}_2\text{O}_8$  in 1 M  $\text{H}_2\text{SO}_4$  (100 ml) at 60 °C for 24 h. After oxidation, the carbon powder was washed with distilled water until all sulfates were removed, which was determined by titrating the filtered solution with  $\text{BaCl}_2$ . Finally, the sample was dried under vacuum.

### Material characterization

Carbon percentages of the treated and untreated graphite samples were determined by heat treating at 950 °C for 3 h in a muffle furnace, according to ASTM-C 561. X-ray diffraction was used to identify the crystalline structure, impurity phases, and the effect of surface modification (XRD, Siemens

D5000). Effects of purification and surface modification morphology of the graphite was observed using Scanning Electron Microscopy (SEM, FEI Quanta 200 FEG-ESEM). Thermogravimetric measurements of raw and treated graphite were taken between 25 and 800 °C under nitrogen atmosphere (Perkin-Elmer TGS-2 Thermogravimetric System). Nicolet 6700 Fourier-transform infrared spectroscopy (FT-IR) was used to analyze the surface structure of purified and surface-modified graphite in the  $400\text{--}4000\text{-cm}^{-1}$  region for absorption mode. The d.c. four probe electrical conductivity measurements were performed on the uniaxially pressed dense pellets between room temperature (25 °C) and 200 °C.

### Electrochemical analysis

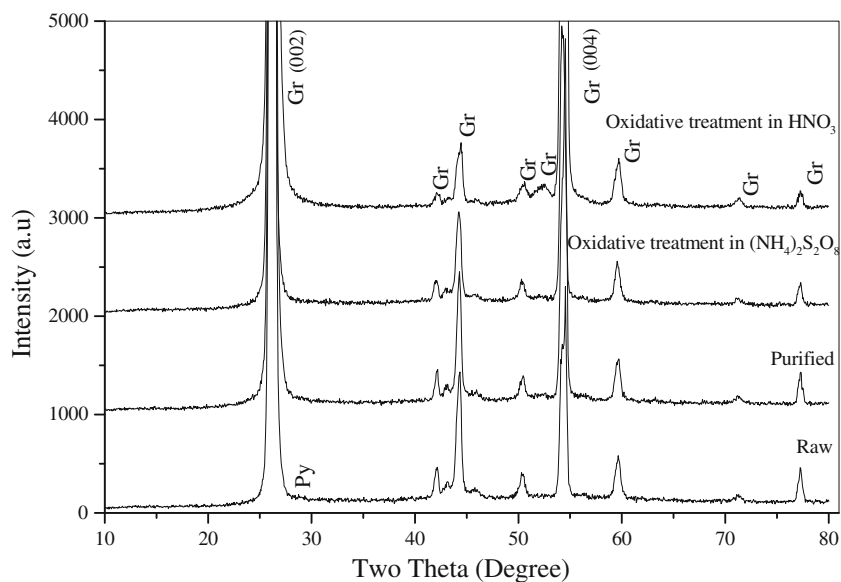
Coin Cells (CR 2032) were assembled in an argon-filled glovebox (Lab Start 50). In order to study the electrochemical properties of the prepared graphite electrode materials, lithium foil (Sigma-Aldrich) was used as a standard counter and reference electrode for all test cells. Electrode was prepared by casting a mixture of 90% of active material (developed vein graphite) and 15% of PvdF (KynarFlex 2801) binder together with acetone (Sigma-Aldrich) solvent on a copper current collector. Circular disks of 12-mm diameter and approximately 100  $\mu\text{m}$  thickness, punched from the fabricated electrodes, were used as working electrodes. The electrolyte was 1 M  $\text{LiPF}_6$  in ethylene carbonate (EC)/diethyl carbonate (DEC)/dimethyl carbonate (DMC) (1:1:1 wt.%) (LP71, BASF, USA). Microporous membranes, Celgard 2400, were used as the separator. Finally, the charge-discharge study of the assembled cells was carried out at C/5 rate with a cutoff voltage of 0.002–1.5 V at room temperature using a Metrohm Auto Lab (PGSTAT302N) controlled by Nova 1.1 program.

## Results and discussion

### Purification and surface modification of vein graphite

NPG sample with initial average carbon percentage of 99.83% was improved to 99.98% after treatment with 5 vol.% HCl. Figure 1 shows the X-ray diffractograms obtained on NPG powders before and after acid leaching purification and after surface modification with  $(\text{NH}_4)_2\text{S}_2\text{O}_8$  and  $\text{HNO}_3$ . The diffraction pattern of the powdered sample exhibits well-developed peaks, indicating the high crystallinity of graphite powder. It can be clearly seen that the diffraction peaks corresponding to the impurity phases were eliminated after the purification process. XRD diffractograms of raw NPG show a small diffraction peak related to pyrite. This peak is absent in purified NPG. Furthermore, the diffractograms clearly indicate that the purification and mild chemical oxidation of the graphite powder do not affect the crystallographic structure of

**Fig. 1** The X-ray diffractograms obtained on NPG before and after the acid leaching purification and after surface modification with  $(\text{NH}_4)_2\text{S}_2\text{O}_8$  and  $\text{HNO}_3$

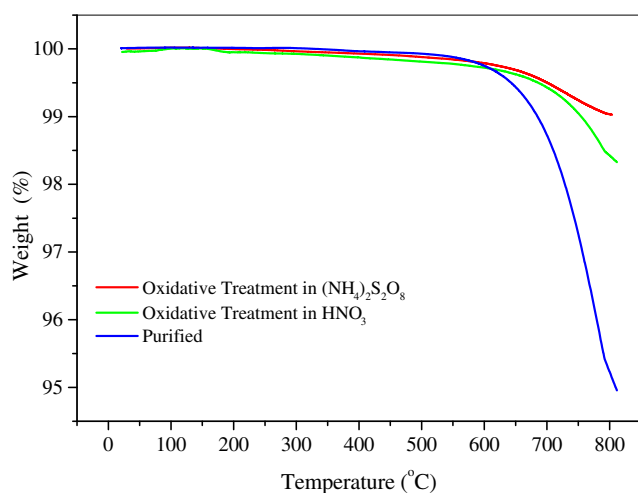


NPG powder and do not involve the formation of an intermediary graphite intercalation compound or other secondary phases [12–14].

Thermogravimetric analysis was also used to investigate the effect of mild oxidation of purified NPG. Figure 2 shows the TGA of the purified NPG before and after the mild oxidation in air and the chemical oxidation. TGA results suggest that the temperature at which combustion began to increase after the chemical oxidation compared to the purified NPG. The more reactive component in the carbon mixture will oxidize at lower ignition temperature [23, 24]. Therefore, mild chemical oxidation leads to a stabilization of the graphite structure due to elimination of some reactive structural imperfections at the graphite surface [16, 19]. Consequently, the

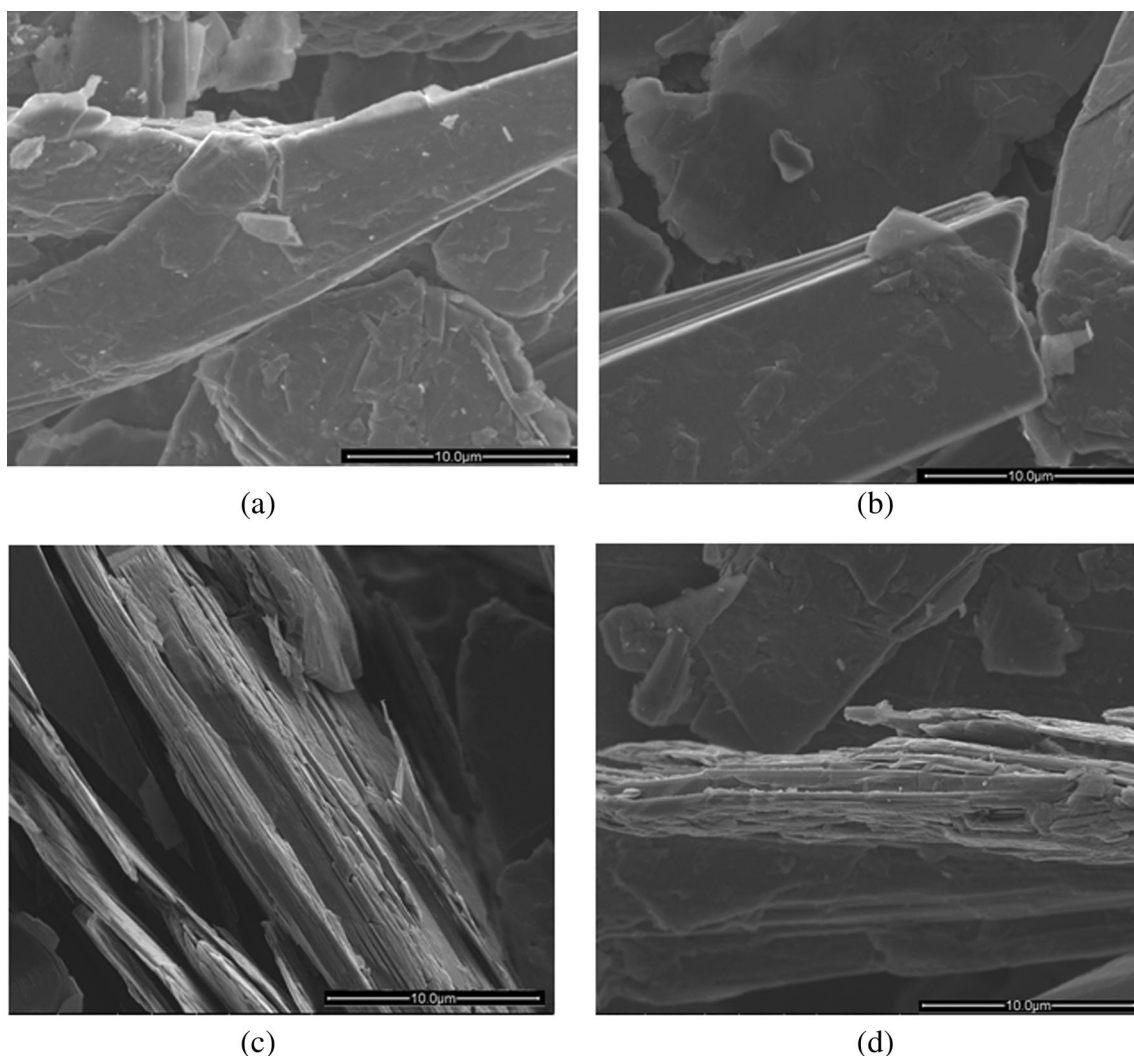
temperature of combustion started to shift to high temperatures after mild oxidation treatments as evident by TGA data. The modified NPG samples exhibit decreased values of weight loss of about 0.5 to 1.7 wt.% compared to the purified NPG (4.75 wt.%). The decreased values suggest a lower concentration of functional groups on the graphite surface [19]. Relating to the previous results, it seems that a decreased amount of surface “defects” and possible removal of surface impurities by mild oxidation treatment leads to a thermally more stable graphite surface structure [19]. The oxidation ability of chemical oxidants governs the formation of oxidizing species on the graphite surface [25]. Combustion began at a higher temperature, 659 °C, for mild oxidized NPG chemically oxidized with  $(\text{NH}_4)_2\text{S}_2\text{O}_8$  compared to that oxidized by  $\text{HNO}_3$  (611 °C).

Figure 3 shows the SEM images of raw, purified, and mildly oxidized NPG (purified) by chemical oxidation. These SEM images indicate some improvement of surface morphology of the mild oxidized graphite samples compared to raw and purified NPG sample. Generally, this surface inhomogeneity is reduced due to attacks on structural imperfection such as edge atoms and carbon chain by the oxidation process. The FT-IR technique is used widely to identify the formation of acidic groups or an oxide layer on the graphite surface [13, 15, 18]. FT-IR spectra of the purified NPG and mild oxidized NPG by chemical oxidation using NO and NS methods are shown in Fig. 4. In the FT-IR spectra, the broad band between 3500 and 3100  $\text{cm}^{-1}$  is attributed to the bending mode of the molecular water. The band at 2330  $\text{cm}^{-1}$  can be assigned to  $\text{CO}_2$  in the gas phase physically adsorbed on the material surface. The purified NPG (prior to oxidation) spectrum shows no significant features apart from the weak absorption band owing to  $\nu_{\text{C}=\text{C}}$  stretching at 1645  $\text{cm}^{-1}$  and a doublet



**Fig. 2** Thermogravimetric (TG) curve for NPG before and after the acid leaching purification and after surface modification with  $(\text{NH}_4)_2\text{S}_2\text{O}_8$  and  $\text{HNO}_3$





**Fig. 3** SEM image of the of NPG (a) before purification and (b) after acid leaching purification (c) after chemical oxidation in  $(\text{NH}_4)_2\text{S}_2\text{O}_8$ , (d) after chemical oxidation in  $\text{HNO}_3$

band at  $2921$  and  $2850\text{ cm}^{-1}$  corresponding to the presence of aliphatic C–H bonds. However, mild oxidized NPG by

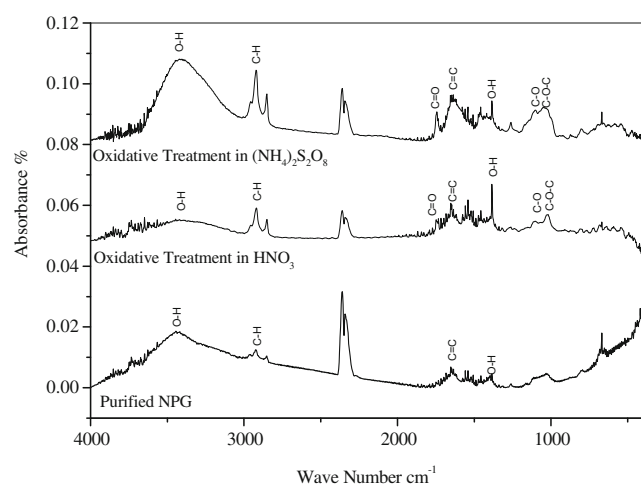


**Fig. 4** FT-IR spectra of the purified and surface modified NPG

chemical oxidation using NO and NS methods shows evidence of formation of carboxylic acid groups on the surface of graphite [13]. Vibrational bands corresponding to  $\nu_{\text{C=O}}$  stretching at  $1720\text{--}1680\text{ cm}^{-1}$ ,  $\nu_{\text{O-H}}$  stretching at  $1360\text{ cm}^{-1}$  and  $\nu_{\text{C-O}}$  stretching at  $1260\text{--}1100\text{ cm}^{-1}$  imply the formation of carbonyl groups, alcoholic phenolic groups, and single C–O groups respectively. Further, a wide, weak band corresponding to  $\nu_{\text{(C-O-C)}}$  appears around  $1000\text{ cm}^{-1}$ . Therefore, the FT-IR spectrum clearly shows the formation of acidic groups or an oxide layer on the surface of the graphite surface after the mild oxidation.

### Electrical conductivity of graphite and graphite electrodes

The electrical conductivity of dense pellets and sheet conductivity of graphite electrodes prepared by graphite powder are given in Table 1. D.C. electrical conductivity measurements of

**Table 1** D.C. electrical conductivity of dense pellets and sheet conductivity of graphite electrodes prepared using graphite powder

Treatment	Electrical conductivity ( $\text{Scm}^{-1}$ )	
	Dense pellet	Electrode
NPG	5.59	0.97
Purified NPG	8.23	1.21
Purified NPG after chemical oxidation with $(\text{NH}_4)_2\text{S}_2\text{O}_8$	4.59	1.45
Purified NPG after chemical oxidation with $\text{HNO}_3$	4.25	0.98

the graphite powders show the semiconducting behavior. They are suggestive that a sufficient electrical conductivity value could be obtained for the anode application. Furthermore, they show that the mild oxidation has not caused any adverse effect on the electronic properties of graphite. The sheet conductivity of graphite electrodes is lower than the D.C. conductivity of the graphite pellets due to the effect of the binder used for the preparation of electrodes.

### Electrochemical performance

Thermogravimetric analysis, studies of surface morphology by scanning electron micrographs and surface analysis by FT-IR measurements, imply that the chemical oxidation with strong oxidizing agents effectively modifies the graphite surface structure. Therefore, the electrochemical performance of raw NPG, purified NPG, and chemically oxidized NPG by NS and NO methods was studied. Table 2 summarizes the results of the charge-discharge study conducted using the NPG at a 0.2 C rate between 0.002 and 1.5 V.

The initial discharge capacity of raw NPG was  $317 \text{ mAh g}^{-1}$  with an irreversible capacity of  $49 \text{ mAh g}^{-1}$  and coulombic efficiency of 84%. For the cells where the graphite had been purified by acid leaching, the discharge capacity of NPG increased slightly to  $327 \text{ mAh g}^{-1}$  with an irreversible capacity of  $39 \text{ mAh g}^{-1}$  and coulombic efficiency of 87%. For cells with purified NPG by chemical oxidation, the discharge capacity increased to  $341 \text{ mAh g}^{-1}$  (NO) and  $345 \text{ mAh g}^{-1}$  (NS), the irreversible capacity decreased from 39 to  $27 \text{ mAh g}^{-1}$  (NO) and  $19 \text{ mAh g}^{-1}$  (NS). The coulombic efficiency in the first cycle increased from 87 to 91% (NO) and 94% (NS), respectively. As indicated in TG and SEM

analyses, some reactive structural imperfections were eliminated effectively during the chemical oxidation. In addition, the surface of NPG was covered with a fresh and dense layer of oxides mainly hydroxyl/phenol, ether, and ester as indicated by the FT-IR data of chemically oxidized graphite. This layer acted as a part of SEI when lithium intercalated and blocked the co-intercalation of solvated  $\text{Li}^+$  [15–25]. As a result, the coulombic efficiency increased after the chemical oxidation.

The first cycle charge-discharge curves of the raw NPG, purified NPG, and chemically oxidized NPG by NS and NO methods are illustrated in Fig. 5. Raw NPG shows a plateau near 0.80–0.90 V vs.  $\text{Li/Li}^+$  which is a characteristic of a formation of an SEI film on the graphite surface and solvent decomposition [11–13]. Hence, impurities in raw NPG, surface imperfections, and defects as evident by XRD, SEM, and TG data may result in solvent decomposition that lead to the above plateau. The extent of the plateau near 0.80–0.90 V vs.  $\text{Li/Li}^+$  gets reduced or disappears after the chemical purification and chemical oxidations (point B in Fig. 5). It maybe due to removing impurities and surface imperfections as evident by TG, SEM, and chemical analysis which lead to solvent decomposition. Moreover, dense oxide layer on the graphite surface as evident by FT-IR data may lead to formation of effective SEI layer during the first cycle [13, 16, 19]. The plateau between about 0.4 and 0.20 V vs.  $\text{Li/Li}^+$  is related to the exfoliation of graphite due to co-insertion of solvent molecules, with lithium migration between graphene layers [11–13]. It can be clearly seen that the exfoliation have reduced after the purification and surface modification. After that, the voltage gradually decreases with the lithium intercalation. Three stages for the lithium intercalation of graphite

**Table 2** Results of first cycle charge-discharge study conducted using the NPG at a 0.2 C rate between 0.002 and 1.5 V

	Discharge capacity ( $\text{mAh g}^{-1}$ )	Charge capacity ( $\text{mAh g}^{-1}$ )	Efficiency (%)	Irreversible capacity ( $\text{mAh g}^{-1}$ )
NPG	317.6	267.8	84.3	49.8
Purified NPG	327.6	287.5	87.8	39.7
NPG NS	345.4	326.1	94.4	19.2
NPG NO	341.4	313.5	91.8	27.9

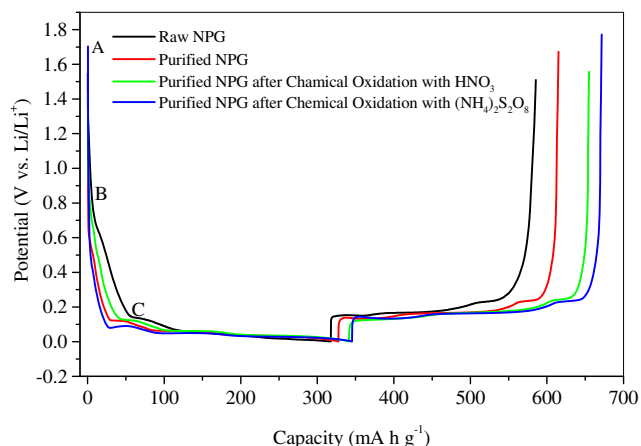


**Fig. 5** Discharge and charge profiles in the first cycle of the natural vein graphite of NPG type before and after treatment at C/5 current rate between 0.002 and 1.5 V

electrode can be identified below 0.20 V vs. Li/Li<sup>+</sup> that corresponds to different stages of Li intercalation.

Cycling behavior of raw NPG, purified NPG, and chemically oxidized NPG by NS and NO methods are illustrated in Fig. 6. In the case of natural graphite, the discharge capacity faded rapidly from 317 to 199 mAh g<sup>-1</sup>. After the purification with the acid leaching process, the discharge capacity of NPG faded from 327 to 227 mAh g<sup>-1</sup>. It can be clearly seen that the rate of capacity fading reduces after the 7th cycle compared to the raw NPG. The discharge capacity of purified NPG oxidized with HNO<sub>3</sub> decreases from 341 to 247 mAh g<sup>-1</sup> over the 10 cycles. The best cycling behavior was found for the chemically oxidized NPG with the strong oxidative agent, (NH<sub>4</sub>)<sub>2</sub>S<sub>2</sub>O<sub>8</sub> where the discharge capacity faded from 345 to 309 mAh g<sup>-1</sup> over 10 cycles. It is interesting to note that the coulombic efficiency of the 10th cycles was 99.9 and 99.6%, respectively, for the purified NPG oxidized with the NS and NO methods.

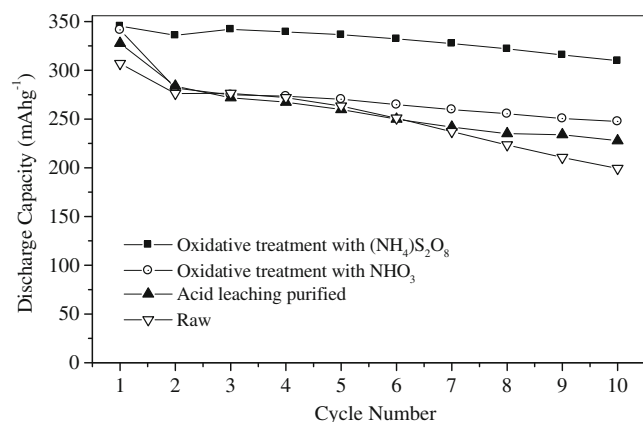


**Fig. 6** Cycling behavior of NPG before and after treatment at C/5 current rate between 0.002 and 1.5 V

## Conclusion

The treatment of purified vein graphite with oxidative solutions of (NH<sub>4</sub>)<sub>2</sub>S<sub>2</sub>O<sub>8</sub> and HNO<sub>3</sub> resulted in a marked improvement of the electrochemical performance as anode materials for LIB. The increased stability of the graphite surface by elimination of imperfections with high activities towards lithium and the formation of dense layers of oxides on the graphite surface is responsible for such improvements. As a result the reactivity of the surface decreases, the decomposition of electrolyte molecules is blocked, and matrices for lithium storage and inlets and outlets for lithium intercalation and deintercalation increases. Therefore, the reversible capacity of raw NPG increases from 317 to 354 mAh g<sup>-1</sup>; the coulombic efficiency in the first cycle increases from 84 to 94% with improved cycling performance after purification and mild surface oxidation with (NH<sub>4</sub>)<sub>2</sub>S<sub>2</sub>O<sub>8</sub>.

The present study confirms that the tested purification method together with surface modification can be successfully used to enhance the electrochemical properties of vein graphite making it suitable for the anode of LIB. All processes take place in the liquid-solid interface, and hence, the uniformity of the product can be easily controlled. Therefore, vein graphite can be successfully used as an anode active material due to its unique morphology, low cost, and high purity.

**Funding information** This work was supported by Higher Education for Twenty First Century (HETC) grant funded by the Ministry of Higher Education Sri Lanka (grant no. UWU/O-ST/R1).

## References

- Wissler M (2006) Graphite and carbon powders for electrochemical applications. *J Power Sources* 156:142–150
- Balogun M-S, Qiu W, Lyu F, Luo Y, Meng H, Li J, Mai W, Mai L, Tong Y (2016) All-flexible lithium ion battery based on thermally-etched porous carbon cloth anode and cathode. *Nano Energy* 26: 446–455
- Touzain P, Balasooriya N, Bandaranayake K, Descolas-Gros C (2010) Vein graphite from the Bogala and Kahatagaha–Kolongaha mines, Sri Lanka: a possible origin. *Can Mineral* 48: 1373–1384
- Dissanayaka CB, Gunawardena RP, Dinalankara DMSK (1988) Trace elements in vein graphite of Sri Lanka. *Chem Geol* 68:121–128
- Ambrosi A, Chua CK, Khezri B, Sofer Z, Webster RD, Pumera M (2012) Chemically reduced graphene contains inherent metallic impurities present in parent natural and synthetic graphite. *PNAS* 109(32):899–904. <https://doi.org/10.1073/pnas.1205388109>
- Zaghib K, Song X, Guerfi A, Rioux R, Kinoshita K (2003) Purification process of natural graphite as anode for Li-ion batteries: chemical versus thermal. *J Power Sources* 119–121: 8–15



7. Lu XJ, Forssberg E (2002) Preparation of high-purity and low-sulphur graphite from Woxna fine graphite concentrate by alkali roasting. *Miner Eng* 15:755–757
8. Zhao H, Ren J, He X, Li J, Jiang C, Wan C (2007) Purification and carbon-film-coating of natural graphite as anode materials for Li-ion batteries. *Electrochim Acta* 52:6006–6011
9. Amaraweera THNG, Balasooriya NWB, Wijayasinghe HWMAC, Attanayake ANB, Dissanayake MAKL (2013) Purity enhancement of Sri Lankan vein graphite for lithium-ion rechargeable battery anode. *Proceedings to 30th Technical Sessions of Geological Society of Sri Lanka*, pp 101–104
10. Rathnayake RMNM, Wijayasinghe HWMAC, Pitawala HMTGA, Yoshimura M, Huang H-H (2017) Synthesis of graphene oxide and reduced graphene oxide by needle platy natural vein graphite. *Appl Surf Sci* 393:309–331
11. Balasooriya NWB, Touzain P, Bandaranayake PWSK (2007) Capacity improvement of mechanically and chemically treated Sri Lanka natural graphite as an anode material in Li-ion batteries. *Ionics* 13:305–309
12. Balasooriya NWB, Touzain P, Bandaranayake PWSK (2006) Lithium electrochemical intercalation into mechanically and chemically treated Sri Lanka natural graphite. *J Phys Chem Solids* 67: 1213–1217
13. Hewathilake HPTS, Karunaratne N, Wijayasinghe A, Balasooriya NWB, Arof AK (2017) Performance of developed natural vein graphite as the anode material of rechargeable lithium ion batteries. *Ionics* 23(6):1417–1422. <https://doi.org/10.1007/s11581-016-1953-1>
14. Amaraweera THNG, Balasooriya NWB, Wijayasinghe HWMAC, Attanayake ANB, Dissanayake MAKL, Mellander B-E (2014) Development of natural Sri Lankan vein graphite as anode material for lithium ion rechargeable batteries. *Proceedings of the 14th Asian Conference on Solid State Ionics (ACSSI-2014)*, pp 252–259
15. Fu LJ, Liu H, Li C, Wu YP, Rahm E, Holze R, Wu HQ (2006) Surface modifications of electrode materials for lithium ion batteries. *Solid State Sci* 8:113–128
16. Ein-Eli Y, Koch VR (1997) Chemical oxidation: a route to enhanced capacity in Li-ion graphite anodes. *J Electrochem Soc* 144(9):2968–2973
17. Wu YP, Jiang C, Wan C, Holze R (2003) Anode materials for lithium ion batteries by oxidative treatment of common natural graphite. *Solid State Ionics* 156:283–290
18. Kumar PK, Stephan AM, Thayananth P, Subramanian V, Gopukumar S, Renganathan NG (2001) Thermally oxidized graphites as anode for lithium-ion cells. *J Power Sources* 97-98:118–121
19. Placke T, Siozios V, Schmitz R, Lux SF, Bieker P, Colle C (2012) Influence of graphite surface modifications on the ratio of basal plane to “non-basal plane” surface area and on the anode performance in lithium ion batteries. *J Power Sources* 200:83–91
20. Wu YP, Jiang C, Wan C, Holze R (2003) Effects of pretreatment of natural graphite by oxidative solutions on its electrochemical performance as anode material. *Electrochim Acta* 48:867–874
21. Menachem C, Wang Y, Flowers F, Peled E, Greenbaum SG (1998) Characterization of lithiated natural graphite before and after mild oxidation. *J Power Sources* 76(1998):180–185
22. Wang H, Yoshio M (2003) Electrochemical performance of raw natural graphite flakes as an anode material for lithium-ion batteries at the elevated temperature 2003. *Mater Chem Phys* 79(1):76–80
23. Badenhorst H, Focke W (2013) Comparative analysis of graphite oxidation behaviour based on microstructure. *J Nucl Mater* 442:75–82
24. Xiaowei L, Jean-Charles R, Suyuan Y (2004) Effect of temperature on graphite oxidation behavior. *Nucl Eng Des* 227:273–280
25. Wu YP, Jianga C, Wana C, Holze R (2002) Modified natural graphite as anode material for lithium ion batteries. *J Power Sources* 111: 329–334